π-Hydrogen Bonding of Aromatics on the Surface of Aerosols: Insights from *Ab Initio* and Molecular Dynamics Simulation

Ya-Juan Feng,[†] Teng Huang,[†] Chao Wang,[‡] Yi-Rong Liu,[†] Shuai Jiang,[†] Shou-Kui Miao,[†] Jiao Chen,[†] and Wei Huang*,[†,§,∥]

[†]Laboratory of Atmospheric Physico-Chemistry, Anhui Institute of Opttics & Fine Mechanics, Chinese Academy of Sciences, Hefei, Anhui 230031, China

[‡]Key Laboratory of Neutronics and Radiation Safety, Institute of Nuclear Energy Safety Technology, Chinese Academy of Sciences, Hefei, Anhui 230031, China

[§]School of Environmental Science & Optoelectronic Technology, University of Science and Technology of China, Hefei, Anhui 230026, China

[∥]CAS Center for Excellence in Urban Atmospheric Environment, Xiamen, Fujian 361021, China

ABSTRACT: Molecular level insight into the interaction between volatile organic compounds (VOCs) and aerosols is crucial for improvement of atmospheric chemistry models. In this paper, the interaction between adsorbed toluene, one of the most significant VOCs in the urban atmosphere, and the aqueous surface of aerosols was studied by means of combined molecular dynamics simulations and *ab initio* quantum chemistry calculations. It is revealed that toluene can be stably adsorbed on the surface of aqueous droplets via hydroxyl−π hydrogen bonding between the H atoms of the water molecules and the C atoms in the aromatic ring. Further, significant modifications on the electrostatic potential map and frontier molecular orbital are induced by the solvation effect of surface water molecules, which would affect the reactivity and pathway of the atmospheric photooxidation of toluene. This study demonstrates that the surface interactions should be taken into consideration in the atmospheric chemical models on oxidation of aromatics.
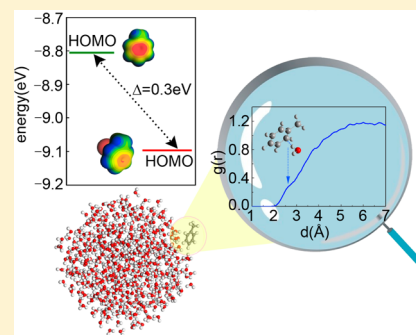
INTRODUCTION

Aromatic hydrocarbons, emitted from fuel-based vehicles, solvent, and other various industrial activities, constitute a significant fraction of the total volatile organic compounds (VOCs) in urban atmospheres.[1−3] According to field measurements, volatile aromatic hydrocarbons constitute up to 30% of the urban volatile hydrocarbon mixture,[4] and benzene, toluene, xylenes, ethylbenzene, and 1,2,4-trimethylbenzene make up more than one-half of them.[5] Furthermore, the aromatic content is dominantly responsible for the secondary organic aerosol (SOA) forming potential of fuel.[1] The atmospheric oxidations of aromatic hydrocarbons in the atmosphere form various nonvolatile and semivolatile organic compounds, playing essential roles in the formation of urban SOAs.[6−8] Hence, the atmospheric chemistry of aromatics is vitally important for understanding the formation of urban SOAs.

Some atmospheric chemistry models have been proposed to describe the atmospheric oxidation of aromatics,[9] which specifically focus on toluene, one of the most abundant aromatic VOCs in urban air (in the range from 1 to 200 ppb) and with the highest aerosol-forming potential among the aromatic hydrocarbons in gasoline vapors.[10] The oxidation of toluene is initiated with attack from electrophiles such as OH radicals in the atmosphere.[11−13] Previous studies have indicated that, largely depending on the initial OH radical attacking site, a variety of ring-opening (e.g., glyoxal and methylglyoxal) and ring-retaining (e.g., benzaldehyde and cresol) products with different aerosol-forming potentials are generated in the oxidation of aromatic VOCs.[14,15]

Previous studies indicate that the aqueous surfaces of aerosols offer a favorable place for some important atmospheric reactions including oxidation of VOCs,[16−20] partially due to the great affinity toward the air/water interface of some organic compounds in the atmosphere and the modification on the electronic structure induced by interfacial interaction.[21−25] Although aromatic molecules are typically classified as hydrophobic, some experimental and theoretical investigations imply that the polarizability of the π-electron cloud admits the possibility of hydration at the ring surface interacting with heteroatoms.[26] For the benzene−water complex, a typical aromatic−water system, a clear manifestation of hydroxyl−π hydrogen bonding has been presented.[26−31] However, the detailed information on the adsorption of atmospheric aromatic molecules with alkyl groups, such as toluene, xylenes, ethylbenzene, and 1,2,4-trimethylbenzene which are dominantly responsible for the SOA formation, remain unclear. The

hydrophobic hydration of toluene can serve as a model for many atmospheric aromatics containing delocalized π-electron and alkyl group systems.

Although much experimental research focused on chemistry at the air/water interface,[16,19,21,22] some molecular level information on the interface interaction, such as adsorption orientation and electronic structure modification, can hardly be fetched via current experiment techniques. On the other hand, theoretical methods, including quantum chemistry calculation, molecular dynamics (MD), and Mont Carlo (MC) simulation, are increasingly utilized to understand the air/water interface interaction and reaction mechanisms in the molecular scale.[32,33] Here, MD simulations and *ab initio* quantum chemistry calculations were combined to provide a molecular level insight into the mechanism of the interaction between toluene and the aqueous surface of aerosols.

■ METHODS

MD Simulations. The classical MD simulations aimed at obtaining the distribution, orientation, and free energy profile of toluene at the interface between small water droplets and air. Molecular dynamics calculations have been performed at 298 K in the NVT ensemble, with the temperature being controlled by a Nosé–Hoover thermostat.[34,35] All the bonding and nonbonding interactions were described by the consistent-valence force field (CVFF).[36] This approach has been successfully used in a previous MD study of hydroxyl–π bonding interaction between benzene and liquid water[28] and has been validated by comparing the *ab initio* calculated geometries to the experimental structures for benzene–water[28,31] and benzene–phenol clusters.[37] The atomic positions were propagated using the velocity-Verlet algorithm with a time step of 0.5 fs. The length of the time step has been tested to be sure to produce a sufficiently accurate trajectory for this system with the least computation costs. The first step of the MD simulation research was to obtain a pure spherical water droplet with a diameter of about 30 Å. Initially 512 water molecules were placed on a uniform $8 \times 8 \times 8$ cubic grid. The distance between nearest water molecules is 1 Å. Then, the cubic water cluster was equilibrated at a temperature of 298 K for 200 ps. The fully relaxed spherical water droplet is shown in Figure 1. Next, a toluene molecule was attached on the surface of the prerelaxed water droplet and unconstrained trajectories of 2.5 ns were carried out at 298 K. The Gibbs free energy profile upon toluene reaching the interface was computed using the umbrella sampling[38] and weighted histogram analysis method (WHAM).[38] The reaction coordinate was taken as the distance between the mass centers of the toluene molecule
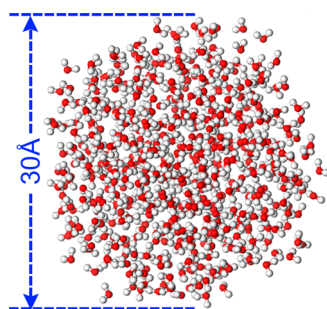
and the water droplet, whose mass center was set as 0 in the reaction coordinate. The reaction coordinate varied from 24 to 14 Å by steps of 0.5 Å, and the bias potential force constant was set to 10 kcal·mol^{-1}·Å^2. The trajectory at each point of the reaction coordinate was carried out for 2.0 ns after full thermalization of 0.5 ns.

***Ab Initio* Geometry Optimization and Electronic Property Calculations.** The second-order Møller–Plesset perturbation (MP2)[39] method was employed for the geometry optimizations and electronic property calculations of the toluene–water complex, because it has, in large part, remedied the limitation of the HF and Kohn–Sham DFT in describing the long-range nonbonded interaction involving electron correlation, which dominates hydroxyl–π hydrogen bonding between aromatics and water.[31,40] Since diffuse functions are important for a precise long-range description of weakly interacting systems, the aug-cc-pVTZ basis set is adopted.[40] A toluene–water complex model was built to understand the nature of the hydroxyl–π hydrogen bonding interaction between toluene and the aqueous surface. The geometry optimizations of the toluene–water complex and electronic property calculations, including the reduced electron density gradient (RDG),[41] ESP surfaces, and frontier molecular orbital, were all performed with the Gaussian 09[42] program package.

■ RESULTS AND DISCUSSION

Although toluene is usually regarded as a typical hydrophobic molecule, experimental and theoretical research has implied that hydroxyl–π hydrogen bonding, analogous to regular hydrogen bonding, could form between the aromatic ring and the OH group, with energetic benefit of approximately 1 kcal·mol^{-1}.[26–31] Indeed, the geometry optimization with the MP2 method demonstrates a stable configuration of the toluene–water complex, displayed in Figure 2a. The bond length of the hydroxyl–π hydrogen bond in the optimized configuration is
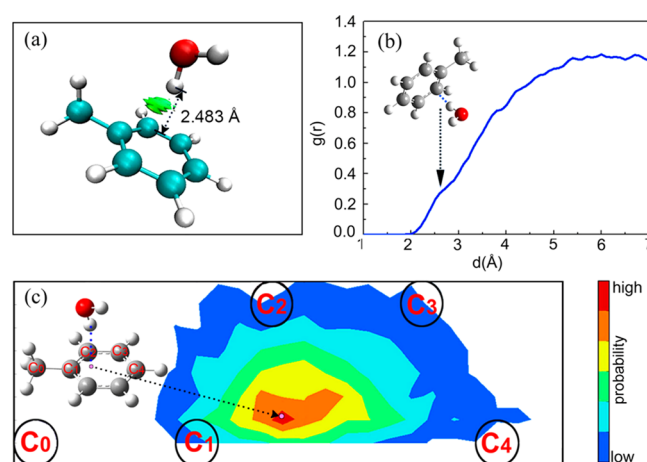
Figure 2. (a) The MP2-optimized configuration of the toluene–water complex and RDG isosurface around the hydroxyl–π hydrogen bond. The distance between the nearest interacting water H and toluene C atoms is also shown. (b) RDF for the hydroxyl–π bonding between H atoms of water and C atoms at the ortho-positions of toluene. The inset is the configuration of the toluene–water complex optimized with MP2. (c) The contour for the distribution of the neighboring hydrogen atoms' projection onto the aromatic plane. The inset is the MP2-optimized configuration of the toluene–water complex, in which the neighboring hydrogen atoms' projection is labeled with a solid pink circle in the aromatic plane.

Figure 1. Snapshot of the fully relaxed droplet consisting of 512 water molecules at $T = 298$ K.
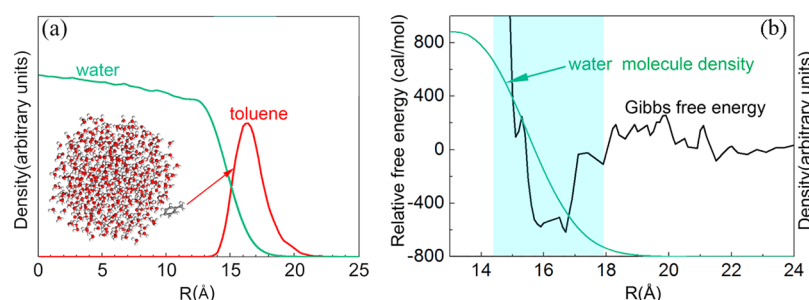
Figure 3. (a) Molecular densities of the centers of mass of water (green line) and toluene (red line) from the MD simulation. (b) Gibbs free energy profile around the air/water droplet interface, and the molecular density of water was also plotted to illustrate the interface area. $R = 0$ corresponds to the center of mass of the water droplet in both parts a and b.
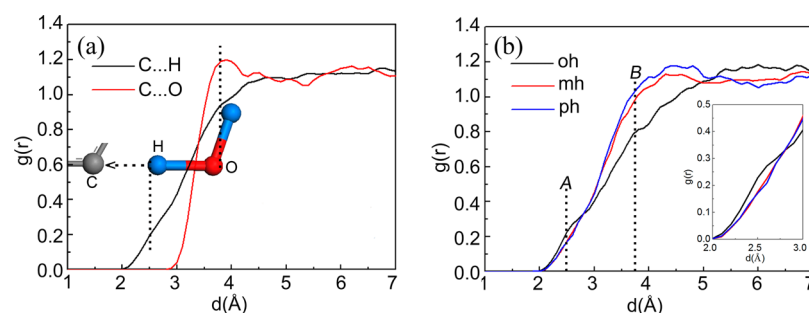

Figure 4. Toluene−water radial distribution functions at the water droplets calculated from MD simulation. (a) The RDFs for the hydroxyl−π bonding between H atoms of water and C atoms (C···H, black line) and between O atoms of water and C atoms (C···O, red line). The ball-and-stick model demonstrates the preferred orientation of the water molecules in the nearest hydration shell. (b) RDF for the hydroxyl−π bonding between H atoms of water and C atoms at the ortho- (oh, black line), meta- (mh, red line), and para- (ph, blue line) positions of toluene. The inset in part b gives the amplificatory RDFs for the hydroxyl−π bonding interactions.

2.483 Å. Moreover, the reduced electron density gradient (RDG) isosurface lying between the interacting C atom of the toluene and the H atom of water also indicates noncovalent attractive interaction.[41] In addition, the structural information on the hydroxyl−π hydrogen bond is also extracted from the 40 000 snapshots of the unconstrained MD trajectory. Since the MD simulation is actually random walking around stable configurations in the potential energy surface, the probability distributions of some geometry parameters can be used to reveal the structure of the hydroxyl−π hydrogen bond. The contour for the spatial distribution of the closely (distance ≤2.9 Å) interacting hydrogen atom projection onto the plane of the aromatic ring is shown in Figure 2c. The projection (labeled as a solid pink circle) of the hydrogen atom involved in the hydroxyl−π hydrogen bonding in the MP2 optimized configuration is also displayed for comparison. It is clear that the H atom projection in the MP2 optimized toluene−water complex is just on the center of the highest probability region of the MD simulation results. Moreover, the radial distribution function (RDF) calculated from MD simulations (Figure 2b) demonstrates the formation of a C (toluene)−H (water) bond at about 2.50 Å from the carbon in the aromatic ring, which is consistent with the MP2 calculated value equal to 2.483 Å. The good agreements in geometries (including spatial and radial distributions of the hydroxyl−π bonding) of the MD and *ab initio* results indicate that MD simulation with a classical force field could well describe the long-range interaction between aromatics and water. This can be interpreted by the fact that the hydroxyl−π hydrogen bonding involves dispersion-like attraction, electrostatic interaction, polarization, and charge transfer, and the binding energy is dominated by the dispersion-like interaction, which is included in empirical potential MD

simulation but underestimated in the HF and Kohn−Sham DFT methods.[43] Similarly, Jaebeom Han and co-workers also demonstrated that, for the benzene−phenol system, the classical potential MD simulations are in good accord with CCSD(T)/CBS, the highest level of the quantum chemistry electronic structure calculations.[37]

Due to the hydroxyl−π hydrogen bond between toluene and the aqueous surface, the toluene molecule moved around the interface of the water droplet within a layer of approximately 4 Å, as shown by the molecular density profiles in Figure 3a. The hydroxyl−π hydrogen bonds formed between the C atoms in the aromatic ring and the H atoms at the water droplet interface contribute to lowering the energy of the system, whereas the interaction between the hydrophobic methyl group and the aqueous surface will induce an energy increase. On the extremely curved surface of small aerosols, it is possible for the C atom in the aromatic ring to be associated with the aqueous surface and for the hydrophobic methyl group to be apart from the surface, resulting in an overall reduction in the free energy. Accordingly, the Gibbs free energy profile upon reaching the interface in Figure 3b exhibits a minimum at the interface area about 16.5 Å from the mass center of the water droplet, responding to the stable adsorbed state. The Gibbs free energy difference between the interface and the gas phase was estimated to be approximately 0.5 kcal·mol^{-1}, in rough agreement with the hydrogen bonding energy of the toluene−water complex predicted by the MP2 method in this work (0.43 kcal·mol^{-1}) and previously reported hydrate energy in the toluene−water (0.89 kcal·mol^{-1})[44] and toluene−phenol systems (0.54 kcal·mol^{-1}).[45] For the Gibbs free energy profile, the decrease of free energy from 20.0 to 16.5 Å indicates the formation of a hydroxyl−π hydrogen bond and the increase
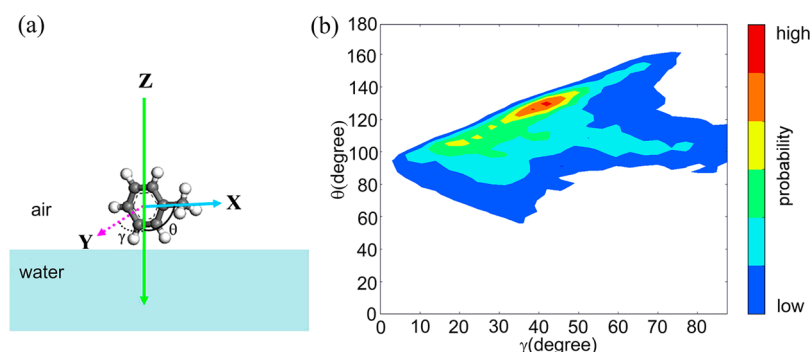
Figure 5. Angular distribution of toluene at the air/water droplet interface.

after 16.0 Å is due to the increase of entropy and the repulsive interaction between water and methyl group.

The distributions of C···H and C···O distances between toluene and water were measured for investigation into the solvation shell. The $g_{CO}(r)$ and $g_{CH}(r)$ distributions for water and toluene interactions are shown in Figure 4a. In the RDF curve of $g_{CO}(r)$, a pronounced peak is located at about 3.7 Å, which corresponds to the O atoms of water in the first aqueous solvation shell. Meanwhile, for the $g_{CH}(r)$ curve, the peak corresponding to the first aqueous solvation shell is shifted into two shoulder peaks around 2.5 and 3.7 Å, corresponding to the hydroxyl−π hydrogen bonded H atom and the H atoms which do not form a hydroxyl−π hydrogen bond with toluene, respectively. The difference between the locations of the first coordination peaks of hydroxyl−π hydrogen bonded O and H atoms in RDF curves indicates a high orientation of the water molecules within the first aqueous solvation shell. If the orientation of water molecules is random, the peaks of the first C···H and C···O coordination shells should be in identical locations (both at 3.7 Å). Instead, the results imply that the O−H bonds of the water molecules in the solution shell prefer pointing toward the C atoms in the aromatic ring, confirming the formation of the hydroxyl−π hydrogen bond, as shown in Figure 4a. Similar behavior was also observed in the aromatics in bulk solution.[26−28]

The RDF curves for the C atoms of toluene at the meta-, para-, and ortho-positions and the H atoms of water in Figure 4b all exhibit the first peak around approximately 2.50 Å (peak A), which corresponds to the hydroxyl−π hydrogen bonding. It is worth noting that the $g(r)$ value of the hydroxyl−π hydrogen bonding of the C atoms at the ortho-positions is significantly higher than those of the C atoms at the meta- and para-positions, indicating a higher potential of hydroxyl−π hydrogen bonding of the C atoms at the ortho-positions. In the coordination peak at around 3.70 Å (peak B) for C atoms and the unbonded H atoms of water in the first aqueous solvation shell, the ortho-positions have the lowest intensity, indicating the least density of unbonded H atoms around the ortho-positions. This could arise from the steric effect of the hydrophobic methyl group, which pushes the highly charged unbonded H atoms of water away. The C atoms at the ortho-positions are much closer to the methyl group than those at the meta- and para-positions. Hence, the steric effect's influence at the ortho-positions is the most significant. In addition, in the MP2 optimized toluene−water complex, the unbonded H atom also stays away from the methyl group (Figure 2a). These results allow it to be concluded that the hydroxyl−π hydrogen bonding at the first solvation shell is much more likely to be

formed between the C atoms at the ortho-positions and the H atoms of water, which may arise from the high electronegativity at the ortho-positions; meanwhile, the steric effect of the hydrophobic methyl group also plays an important role in the configuration of the hydroxyl−π hydrogen bond.
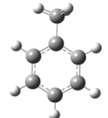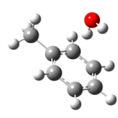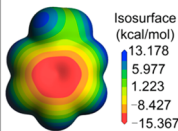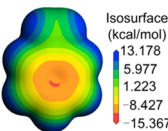
As shown by the angular distribution of toluene at the air/water droplet interface in Figure 5, the orientation of toluene molecules with respect to the air/water interface was sampled from the MD simulation trajectory. In agreement with the orientational preference at the aqueous surfaces observed by Vácha,[46] a clear orientational preference is also observed in our MD trajectories. The orientation of the toluene at the interface can be described with two angles. As displayed in Figure 5a, the X-axis is defined as the axis connecting the center of mass of the toluene molecule and the C atom in the methyl group; the Y-axis is defined as the axis that is perpendicular to the benzene ring; and the Z-axis is defined as the axis connecting the center of mass of the toluene molecule and the center of mass of the entire water droplet. The orientation of the toluene molecule is determined by the θ angle, formed between the Z-axis and the X-axis, and the γ angle, formed between the Z-axis and the Y-axis. The probability distributions of the θ and γ angles are displayed as a pseudocolor map in Figure 5b. Unlike the flat lying of the single benzene molecule in the water slab surface,[46] in our simulation, most of the snapshots are located in the narrow region where the θ angle is between 120 and 140° and the γ angle is between 30 and 50°. For the most favorable position, the toluene is positioned in an inclined manner on the aqueous surface with the meta-, ortho-, and para-positions on the same edge contacting the surface and the methyl group is apart from the aqueous surface. As revealed by the RDF results, the configuration of the hydroxyl−π hydrogen bonded toluene and water is affected by hydroxyl−π hydrogen bonding which pulls the H atom of the interacting water molecules to the C atoms in the aromatic ring and the hydrophobic force which pushes the methyl group away from the water molecule. The orientation of toluene at the droplet surface results from the balance of these two effects. The orientation of toluene at the droplet surface results from the balance of these two effects.

It is well-known that the solvation effects of neighboring water molecules could influence the electronic properties of the solute and hence modify its chemical reactivity. Multiple methods including ESP surface and frontier molecular orbit analysis were employed to discover the chemistry modification on toluene from the hydroxyl−π hydrogen bonded water molecule.

The ESP on the molecular surface is an effective means to analyze and predict noncovalent interactions, such as hydrogen

bonding.[47,48] The ESP surfaces of toluene in the gas phase and toluene−water complex are displayed in Table 1. For both the

Table 1. Configuration of the Toluene Molecule and Toluene−Water Complex Optimized at the MP2/aug-cc-pVTZ Level, Electrostatic Potential Map at the 0.001 Electron au Density Isosurface,[a] and Energies (eV) of the HOMO, LUMO, and HOMO−LUMO Gap

electrostatic potential surface map	Isosurface (kcal/mol) 13.178 5.977 1.223 −8.427 −15.367	Isosurface (kcal/mol) 13.178 5.977 1.223 −8.427 −15.367
HOMO[eV]	−8.806	−9.098
LUMO[eV]	0.8193	0.7099
HOMO-LUMO gap [eV]	9.625	9.808

[a]The electrostatic potential surfaces are scaled from 15.367 kcal mol^{-1} (red) to 13.178 kcal mol^{-1} (blue).

free toluene molecule and the toluene−water complex, there is a region of negative surface potential above and below the ring, arising from the π electrons. However, for the toluene−water complex, an overall shift toward positive on the ESP of the aromatic ring is clearly present, which identifies the electron donor of toluene in the hydroxyl−π hydrogen bonding. A more important modification is the distribution of the local minimum of ESP because the electrophilic attacking usually take place on the site of the local ESP minimums. For the free toluene, the local minimum of ESP almost evenly distributed on the C atoms of the aromatic ring. However, the local minimum of ESP is located around a C atom on the meta-position that is close to the interacting water molecule. The ESP analysis elucidates a marked modification on the ESP of toluene is induced by the hydroxyl−π hydrogen bonding.

In addition, the modification on the chemical properties from interface solvation effects was analyzed by looking at the energy variation of the highest occupied molecular orbital (HOMO) and the lowest unoccupied molecular orbital (LUMO), which determine the potential of bond formation. From Table 1, the orbital gap for the toluene−water model (9.808 eV) is larger than that of the isolated toluene molecule (9.625 eV). The orbital energy of the toluene−water model is influenced by the presence of the water solvent. The uptake process produces a slight decrease of the HOMO and LUMO frontier orbital energies as expected from simple considerations of solvation, predicting enhancement of thermodynamic stability for the toluene at the aqueous surface. Moreover, the molecular orbital diagram could offer a qualitative picture to speculate the reactivity of solvated toluene at the surface with radicals. Figure 6 displays a comparison of HOMO and LUMO energies for OH radical and toluene as a function of the molecular
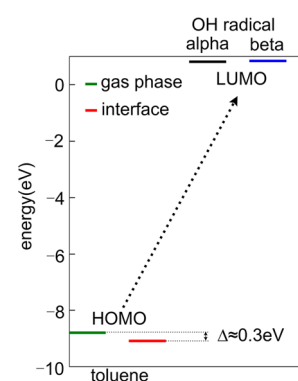
Figure 6. Calculated HOMO and LUMO orbital diagram of the toluene−water complex (red line) and OH radical (black line and blue line). The HOMO of toluene in the gas phase is also plotted for comparison (green line).

environment, free and in toluene−water complex. The interface solvation effects on the HOMO and LUMO energies lead to variation in the electron donor−acceptor capability of the toluene. It is expected that the electron transfer from toluene in the complex to OH might require a higher activation energy than that in the gas phase because the corresponding HOMO (toluene−water complex)−LUMO (OH) gap increases by about 0.3 eV. The acceptor−donor energy difference is the dominant factor determining the overall reactivity of a molecule. It indicates that the oxidation of toluene at the air/water interface initiated by OH attacking is depressed by modification on the electronic structure from hydroxyl−π hydrogen bonding, in good accordance with the ESP analysis.

■ CONCLUSIONS

In summary, our study based on a combination of MD simulation and *ab initio* calculations reveals a molecular level mechanism of the interfacial interaction of toluene and the aqueous surface of aerosols. The results demonstrate that the adsorption of toluene at the air/water interface is dominated by hydroxyl−π hydrogen bonding and the orientation preference is induced by the competition between the heterogeneous attractive interaction of hydroxyl−π hydrogen bonding and the steric effect of the hydrophobic methyl group. Detailed electronic structure calculation on the toluene−water complex reveals that the hydroxyl−π hydrogen bonding induces modification on the distribution of ESP on the molecular surface and on the molecular orbits. The modification could alter the attacking site and reactivity of OH electrophilic addition, and further influence the final products of photo-oxidation and SOA-forming potential. This research shows that the hydroxyl−π hydrogen bonding between aromatics and the aqueous surface of aerosols could induce a marked modification on the chemical properties of aromatics, which should be included in the atmospheric chemistry models of photo-oxidation of aromatics. On the other hand, it should be noticed that the above *ab initio* calculation only reveals the electronic modification induced by the hydroxyl−π hydrogen bonding in the toluene−water complex and other interfacial effects were not covered. The overall electronic modification induced by the aqueous interface would need to be further studied with sophisticated quantum chemistry methods or QM/MM approaches adapted for large scale systems.

■ AUTHOR INFORMATION

Corresponding Author
*E-mail: huangwei6@ustc.edu.cn. Phone: +86-551-65595697. Fax: +86-551-65595697.

Notes
The authors declare no competing financial interest.

■ REFERENCES

(1) Odum, J. R.; Jungkamp, T. P. W.; Griffin, R. J.; Flagan, R. C.; Seinfeld, J. H. The Atmospheric Aerosol-Forming Potential of Whole Gasoline Vapor. *Science* **1997**, *276*, 96−99.

(2) Ansari, A. S.; Pandis, S. N. Water Absorption by Secondary Organic Aerosol and Its Effect on Inorganic Aerosol Behavior. *Environ. Sci. Technol.* **2000**, *34* (1), 71−77.

(3) Karl, T.; Fall, R.; Crutzen, P. J.; Jordan, A.; Lindinger, W. High Concentrations of Reactive Biogenic VOCs at a High Altitude Site in Late Autumn. *Geophys. Res. Lett.* **2001**, *28* (3), 507−510.

(4) Qiu, C.; Khalizov, A. F.; Zhang, R. Soot Aging From OH-Initiated Oxidation of Toluene. *Environ. Sci. Technol.* **2012**, *46* (17), 9464−9472.

(5) Jang, M.; Kamens, R. M. Characterization of Secondary Aerosol from the Photooxidation of Toluene in the Presence of NO$_x$ and 1-Propene. *Environ. Sci. Technol.* **2001**, *35* (18), 3626−3639.

(6) Volkamer, R.; Jimenez, J. L.; San Martini, F.; Dzepina, K.; Zhang, Q.; Salcedo, D.; Molina, L. T.; Worsnop, D. R.; Molina, M. J. Secondary Organic Aerosol Formation From Anthropogenic Air Pollution: Rapid and Higher than Expected. *Geophys. Res. Lett.* **2006**, *33* (17), L17811.

(7) Robinson, A. L.; Donahue, N. M.; Shrivastava, M. K.; Weitkamp, E. A.; Sage, A. M.; Grieshop, A. P.; Lane, T. E.; Pierce, J. R.; Pandis, S. N. Rethinking Organic Aerosols: Semivolatile Emissions and Photochemical Aging. *Science* **2007**, *315* (5816), 1259−1262.

(8) Keyte, I. J.; Harrison, R. M.; Lammel, G. Chemical Reactivity and Long-Range Transport Potential of Polycyclic Aromatic Hydrocarbons-A Review. *Chem. Soc. Rev.* **2013**, *42* (24), 9333−9391.

(9) Hildebrandt Ruiz, L.; Paciga, A.; Cerully, K.; Nenes, A.; Donahue, N.; Pandis, S. Aging of Secondary Organic Aerosol from Small Aromatic VOCs: Changes in Chemical Composition, Volatility and Hygroscopicity. *Atmos. Chem. Phys. Discuss.* **2014**, *14* (22), 31441−31481.

(10) Demirdjian, B.; Rossi, M. The Surface Properties of SOA Generated from Limonene and Toluene Using Specific Molecular Probes: Exploration of A New experimental technique. *Atmos. Chem. Phys. Discuss.* **2005**, *5* (1), 607−654.

(11) Forstner, H. J.; Flagan, R. C.; Seinfeld, J. H. Secondary Organic Aerosol from the Photooxidation of Aromatic Hydrocarbons: Molecular Composition. *Environ. Sci. Technol.* **1997**, *31* (5), 1345−1358.

(12) Molina, M. J.; Zhang, R.; Broekhuizen, K.; Lei, W.; Navarro, R.; Molina, L. T. Experimental Study of Intermediates from OH-Initiated Reactions of Toluene. *J. Am. Chem. Soc.* **1999**, *121* (43), 10225−10226.

(13) Suh, I.; Zhang, R.; Molina, L. T.; Molina, M. J. Oxidation Mechanism of Aromatic Peroxy and Bicyclic Radicals from OH-Toluene Reactions. *J. Am. Chem. Soc.* **2003**, *125* (41), 12655−12665.

(14) Fang, W.; Gong, L.; Shan, X.; Liu, F.; Wang, Z.; Sheng, L. Thermal Desorption/Tunable Vacuum-Ultraviolet Time-of-Flight Photoionization Aerosol Mass Spectrometry for Investigating Secondary Organic Aerosols in Chamber Experiments. *Anal. Chem.* **2011**, *83* (23), 9024−9032.

(15) Andino, J. M.; Smith, J. N.; Flagan, R. C.; Goddard, W. A.; Seinfeld, J. H. Mechanism of Atmospheric Photooxidation of Aromatics: A Theoretical Study. *J. Phys. Chem.* **1996**, *100* (26), 10967−10980.

(16) Donaldson, D.; Valsaraj, K. T. Adsorption and Reaction of Trace Gas-Phase Organic Compounds on Atmospheric Water Film Surfaces: A Critical Review. *Environ. Sci. Technol.* **2010**, *44* (3), 865−873.

(17) Heath, A. A.; Valsaraj, K. T. Effects of Temperature, Oxygen Level, Ionic Strength, and pH on the Reaction of Benzene with Hydroxyl Radicals at the Air-Water Interface in Comparison to the Bulk Aqueous Phase. *J. Phys. Chem. A* **2015**, *119* (31), 8527−8536.

(18) Mmereki, B. T.; Donaldson, D. J.; Gilman, J. B.; Eliason, T. L.; Vaida, V. Kinetics and Products of the Reaction of Gas-Phase Ozone With Anthracene Adsorbed at the Air-Aqueous Interface. *Atmos. Environ.* **2004**, *38* (36), 6091−6103.

(19) Raja, S.; Valsaraj, K. T. Heterogeneous Oxidation by Ozone of Naphthalene Adsorbed at the Air-Water Interface of Micron-Size Water Droplets. *J. Air Waste Manage. Assoc.* **2005**, *55* (9), 1345−1355.

(20) Fu, H.; Ciuraru, R.; Dupart, Y.; Passananti, M.; Tinel, L.; Rossignol, S.; Perrier, S.; Donaldson, D. J.; Chen, J.; George, C. Photosensitized Production of Atmospherically Reactive Organic Compounds at the Air/Aqueous Interface. *J. Am. Chem. Soc.* **2015**, *137* (26), 8348−8351.

(21) Donaldson, D. J.; Anderson, D. Adsorption of Atmospheric Gases at the Air−Water Interface. 2. C$_1$-C$_4$ Alcohols, Acids, and Acetone. *J. Phys. Chem. A* **1999**, *103* (7), 871−876.

(22) Bruant, R. G.; Conklin, M. H. Adsorption of Benzene and Methyl-Substituted Benzenes at the Vapor/Water Interface. 3. Finite Binary-Component VHOC Adsorption. *J. Phys. Chem. B* **2002**, *106* (9), 2232−2239.

(23) Raja, S.; Valsaraj, K. T. Uptake of Aromatic Hydrocarbon Vapors (Benzene and Phenanthrene) at the Air-Water Interface of Micron-size Water Droplets. *J. Air Waste Manage. Assoc.* **2004**, *54* (12), 1550−1559.

(24) Kolb, C. E.; Cox, R. A.; Abbatt, J. P. D.; Ammann, M.; Davis, E. J.; Donaldson, D. J.; Garrett, B. C.; George, C.; Griffiths, P. T.; Hanson, D. R.; et al. An Overview of Current Issues in the Uptake of Atmospheric Trace Gases by Aerosols and Clouds. *Atmos. Chem. Phys.* **2010**, *10* (21), 10561−10605.

(25) Martins-Costa, M. T. C.; Anglada, J. M.; Francisco, J. S.; Ruiz-Lopez, M. F. Reactivity of Volatile Organic Compounds at the Surface of a Water Droplet. *J. Am. Chem. Soc.* **2012**, *134* (28), 11821−11827.

(26) Ravishanker, G.; Mehrotra, P. K.; Mezei, M.; Beveridge, D. L. Aqueous Hydration of Benzene. *J. Am. Chem. Soc.* **1984**, *106* (15), 4102−4108.

(27) Takahashi, H.; Suzuoka, D.; Morita, A. Why is Benzene Soluble in Water? Role of OH/π Interaction in Solvation. *J. Chem. Theory Comput.* **2015**, *11* (3), 1181−1194.

(28) Gierszal, K. P.; Davis, J. G.; Hands, M. D.; Wilcox, D. S.; Slipchenko, L. V.; Ben-Amotz, D. π-Hydrogen Bonding in Liquid Water. *J. Phys. Chem. Lett.* **2011**, *2* (22), 2930−2933.

(29) Zhao, Y.; Tishchenko, O.; Truhlar, D. G. How Well Can Density Functional Methods Describe Hydrogen Bonds to π Acceptors? *J. Phys. Chem. B* **2005**, *109* (41), 19046−19051.

(30) Oki, M.; Iwamura, H. Steric Effects on the O-H···π Interaction in 2-Hydroxybiphenyl. *J. Am. Chem. Soc.* **1967**, *89* (3), 576−579.

(31) Suzuki, S.; Green, P. G.; Bumgarner, R. E.; Dasgupta, S.; Goddard, W. A.; Blake, G. A. Benzene Forms Hydrogen Bonds with Water. *Science* **1992**, *257* (5072), 942−945.

(32) Gerber, R. B.; Varner, M. E.; Hammerich, A. D.; Riikonen, S.; Murdachaew, G.; Shemesh, D.; Finlayson-Pitts, B. J. Computational Studies of Atmospherically-Relevant Chemical Reactions in Water Clusters and on Liquid Water and Ice Surfaces. *Acc. Chem. Res.* **2015**, *48*, 399−406.

(33) Gerber, R. B.; Shemesh, D.; Varner, M. E.; Kalinowski, J.; Hirshberg, B. Ab Initio and Semi-Empirical Molecular Dynamics Simulations of Chemical Reactions in Isolated Molecules and in Clusters. *Phys. Chem. Chem. Phys.* **2014**, *16*, 9760−9775.

(34) Nosé, S. A Unified Formulation of the Constant Temperature Molecular Dynamics Methods. *J. Chem. Phys.* **1984**, *81* (1), 511−519.

(35) Hoover, W. G. Canonical Dynamics-Equilibrium Phase-Space Distributions. *Phys. Rev. A: At., Mol., Opt. Phys.* **1985**, *31* (3), 1695−1697.

(36) Dauberosguthorpe, P.; Roberts, V. A.; Osguthorpe, D. J.; Wolff, J.; Genest, M.; Hagler, A. T. Structure and Energetics of Ligand-Binding to Proteins- Escherichia-Coli Dihydrofolate Reductase Trimethoprim, a Drug-Receptor System. *Proteins: Struct., Funct., Genet.* **1988**, *4*, 31−47.

(37) Kwac, K.; Lee, C.; Jung, Y.; Han, J.; Kwak, K.; Zheng, J.; Fayer, M. D.; Cho, M. Phenol-Benzene Complexation Dynamics: Quantum Chemistry Calculation, Molecular Dynamics Simulations, and Two Dimensional IR Spectroscopy. *J. Chem. Phys.* **2006**, *125* (24), 244508.

(38) Kästner, J. Umbrella Sampling. *Adv. Rev.* **2011**, *00*, 1−11.

(39) Møller, C.; Plesset, M. S. Note on an Approximation Treatment for Many-Electron Systems. *Phys. Rev.* **1934**, *46* (7), 618−622.

(40) Feller, D. Strength of the Benzene-Water Hydrogen Bond. *J. Phys. Chem. A* **1999**, *103* (38), 7558−7561.

(41) Johnson, E. R.; Keinan, S.; Mori-Sánchez, P.; Contreras-García, J.; Cohen, A. J.; Yang, W. Revealing Noncovalent Interactions. *J. Am. Chem. Soc.* **2010**, *132* (18), 6498−6506.

(42) Frisch, M. J.; Trucks, G. W.; Schlegel, H. B.; Scuseria, G. E.; Robb, M. A.; Cheeseman, J. R.; Scalmani, G.; Barone, V.; Mennucci, B.; Petersson, G. A.; et al. *Gaussian 09*; Gaussian, Inc.: Wallingford, CT, 2009.

(43) Chai, J.-D.; Head-Gordon, M. Long-Range Corrected Hybrid Density Functionals with Damped Atom-Atom Dispersion Corrections. *Phys. Chem. Chem. Phys.* **2008**, *10* (44), 6615−6620.

(44) Cabani, S.; Gianni, P.; Mollica, V.; Lepori, L. Group Contributions to the Thermodynamic Properties of Non-ionic Organic Solutes in Dilute Aqueous-Solution. *J. Solution Chem.* **1981**, *10* (8), 563−595.

(45) Yoshida, Z.-i.; Osawa, E. Intermolecular Hydrogen Bond Involving a π-Base as the Proton Acceptor. II. Interaction between Phenol and Various π-Bases. Preliminary Infrared Study. *J. Am. Chem. Soc.* **1965**, *87* (7), 1467−1469.

(46) Vácha, R.; Cwiklik, L.; Řezáč, J.; Hobza, P.; Jungwirth, P.; Valsaraj, K.; Bahr, S.; Kempter, V. Adsorption of Aromatic Hydrocarbons and Ozone at Environmental Aqueous Surfaces. *J. Phys. Chem. A* **2008**, *112* (22), 4942−4950.

(47) Politzer, P.; Murray, J. S.; Concha, M. C. The Complementary Roles of Molecular Surface Electrostatic Potentials and Average Local Ionization Energies With Respect to Electrophilic Processes. *Int. J. Quantum Chem.* **2002**, *88* (1), 19−27.

(48) Murray, J. S.; Politzer, P. The Electrostatic Potential: An Overview. *Wires. Comput. Mol. Sci.* **2011**, *1* (2), 153−163.